European Journal of Chemistry

Journal webpage: www.eurjchem.com

Synthesis and biological evaluation of phthalimide dithiocarbamate and dithioate derivatives as anti-proliferative and anti-angiogenic agents-I

Magdy Zahran [1], Hussein Agwa [1,2,*], Amany Osman [1], Sherif Hammad [2,3], Bishoy El-Aarag [4], Nasser Ismail [5], Tarek Salem [6] and Amira Gamal-Eldeen [7]

[1] *Chemistry Department, Faculty of Science, Menoufia University, Shebin El-Koom, 32511, Egypt*
[2] *Research and Development Department, Pharco B International Company for Pharmaceutical Industries, Borg El-Arab, Alexandria, 21934, Egypt*
[3] *Department of Pharmaceutical Chemistry, Faculty of Pharmacy, Helwan University, Cairo, 11599, Egypt*
[4] *Biochemistry Division, Chemistry Department, Faculty of Science, Menoufia University, Shebin El-Koom, 32511, Egypt*
[5] *Department of Pharmaceutical Chemistry, Faculty of Pharmacy, Ain-Shams University, Cairo, 11599, Egypt*
[6] *Molecular Biology Department, Genetic Engineering and Biotechnology Research Institute (GEBRI), Sadat City University, Sadat City, 32897, Egypt*
[7] *Cancer Biology and Genetics Laboratory, Centre of Excellence for Advanced Sciences, National Research Centre, Dokki, Cairo, 11599, Egypt*

** Corresponding author at: Chemistry Department, Faculty of Science, Menoufia University, Shebin El-Koom, 32511, Egypt.*
Tel.: +2.034.626448. Fax: +2.034.626026. E-mail address: husseinagwa@gmail.com (H. Agwa).

ARTICLE INFORMATION

DOI: 10.5155/eurjchem.8.4.391-399.1652

Received: 15 September 2017
Received in revised form: 23 October 2017
Accepted: 25 October 2017
Published online: 31 December 2017
Printed: 31 December 2017

KEYWORDS

Cytotoxicity
Phthalimide
Thalidomide
Dithiocarbamate
Antitumor activity
Molecular Docking

ABSTRACT

A facile synthesis of new phthalimide dithiocarbamate and dithioate analogs 8a-j, 9a-e and 9g-j were achieved by the reaction of *N*-chloromethyl and *N*-bromoethylphthalimide with carbon disulfide (CS_2) and various amines. The structures of the synthesized analogs were elucidated by spectroscopic methods, including IR, ^{1}H NMR and ^{13}C NMR, and ESI-HRMS techniques. The antiproliferative activity of the newly synthesized compounds was also evaluated against various human cancer cell lines. The compound 9e and 9i exhibited the highest activity against human breast adenocarcinoma MCF-7 and hepatocellular carcinoma HepG2 cells. Compound 8f showed better antiproliferative effect against colon carcinoma HCT-116 and cervical carcinoma HeLa compared to thalidomide. The binding affinity to vascular endothelial growth factor receptor (VEGFR) of some compounds was assessed in addition to molecular docking study. Compounds 9e and 9i showed high docking score values and they significantly declined the concentration of VEGFR.

Cite this: *Eur. J. Chem.* **2017**, *8(4)*, 391-399

1. Introduction

Thalidomide (**TH**, Figure 1), was originally launched in the 1950s as sedative and antiemetic drug and was subsequently withdrawn from the market in 1960s owing to its teratogenic properties [1-3]. Recently, **TH** has attracted a considerable attention due to its pronounced antiangiogenic activity. **TH** has been re-approved by FDA in 2006 and re-purposed in the treatment of various hematological malignancies such as multiple myeloma and solid tumors such as colon, brain, and prostate cancers [4].

TH is considered to be a soft drug yielding biologically active metabolites upon biotransformation. Among these metabolites, phthalimide species represents a pharmacophoric group which might be the reason for their biological activities [5]. Based on these results and assumption, new series of phthalimide derivatives were synthesized and evaluated as potential antitumor drug candidates [6,7]. Recently, our group reported the potency of the thalidomide dithiocarbamate analogs as novel antitumor derivatives [8-14].

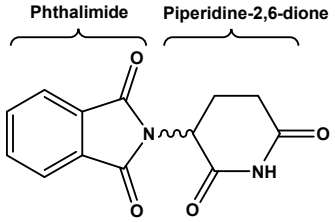

Figure 1. Chemical structure of thalidomide (**TH**).

On the other hand, dithiocarbamic acid esters have drawn a great attention due to their cancer chemopreventive and antitumor activities [15,16].

ISSN 2153-2249 (Print) / ISSN 2153-2257 (Online)
http://dx.doi.org/10.5155/eurjchem.8.4.391-399.1652

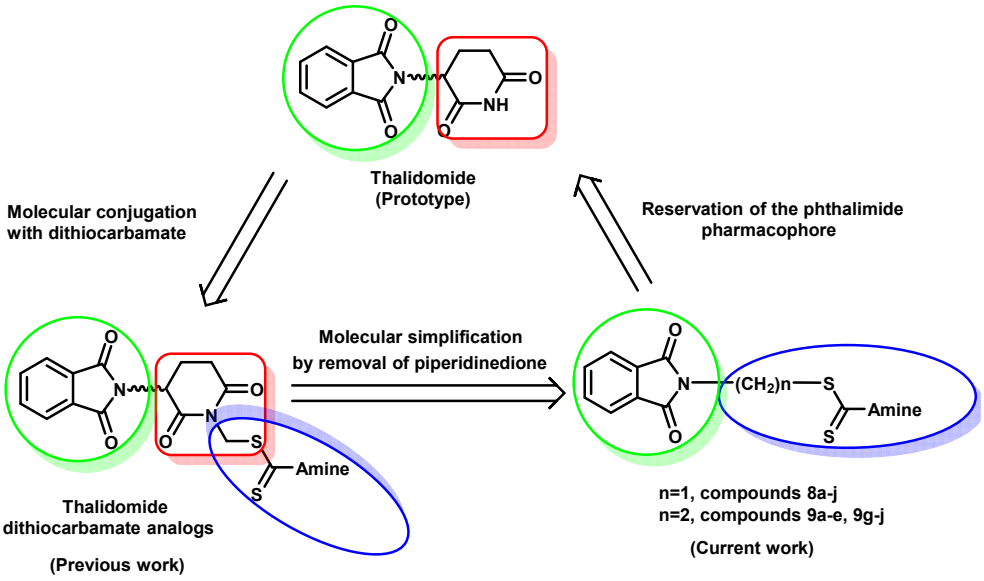

Figure 2. Rational design of the targeted synthesized compounds.

Some molecules that incorporated dithiocarbamic acid ester functionality, as a linker between different pharmacophores, showed significant anticancer activities, such as **TH** derivatives [8-14], chromones [17], quinazolinones [18] and naphthalimide derivatives [19].

Our research interest is still existing in development of **TH** analogs and potential antitumor compounds [8-14,20-22]. So, we herein describe the design, synthesis and biological evaluation of novel dithiocarbamate analogs connected either through methylene or ethylene bridges to phthalimide pharmacophoric core. The insertion of one or two carbon spacers to connect the *N*-terminus of phthalimide with dithiocarbamate groups was executed to explore the influence of excluding the 2,6-piperidinedione moiety from **TH** from one side and the impact of the linker length on antitumor activity from the other side (Figure 2). Moreover, the newly synthesized phthalimide derivatives were evaluated for their growth inhibitory effects against various cancer cell lines. Molecular docking studies as well as their binding affinity on VEGFR were also investigated.

2. Experimental

2.1. Instrumentation

The progress of all reactions and synthesized product were monitored via analytical silica gel thin layer chromatography (TLC) plates 60 F_{254} which were purchased from Merck and spots were located by UV light. ^{1}H and ^{13}C NMR spectra for all synthesized compounds were recorded on a Bruker 400 MHz spectrometer for ^{1}H and 100 MHz for ^{13}C, with TMS as an internal standard for ^{1}H NMR, chemical shifts are reported in parts per million (ppm) relative to the respective deuterated solvent peak $CDCl_3$ (δ 7.27 ppm), DMSO-d_6 (δ 2.50 ppm) for ^{1}H and $CDCl_3$ (δ 77.00 ppm), DMSO-d_6 (δ 39.51 ppm) for ^{13}C NMR. MALDI mass spectra of synthesized compounds were recorded on JEOL JMS-700N for electron ionization or on JEOL JMS-T100TD for electro-spray ionization using α-cyano-4-hydroxycinnamic acid (CHCA) as a matrix (*m/z* 189.17) (Nagasaki University, Japan). Electro-spray ionization high resolution mass spectra (ESI-HRMS) were performed on PE SCIEX API Q-Star Pulsar Mass Spectrometer. For accurate ion mass determinations, the [MH$^+$] or [MNa$^+$] ion was peak matched by calibration with NaI (University of Southern Denmark, Denmark). Infrared (IR) spectra were recorded (KBr) on a Pye-Unicam Sp-883 Perkins-Elmer spectrometer, Micro-analytical Laboratory, Faculty of Science, Cairo University. Melting points were recorded on Stuart scientific melting point apparatus. All chemicals and solvents were purchased from E. Merck (Darmstadt, Germany) and Sigma-Aldrich.

2.2. Synthesis

2.2.1. General procedure for the synthesis of phthalimide dithiocarbamate and dithioate analogs (8a-j, 9a-e, 9g-j)

A solution of carbon disulfide (CS_2) (1 mL) and different amines (1 equivalent) in acetonitrile (CH_3CN) (5 mL) was stirred for 30 min at room temperature. *N*-chloromethyl phthalimide (**3**) or *N*-bromoethylphthalimide (**7**) (1 equivalent) was added to the resulting mixture and the stirring was continued for 48 h. The reaction was monitored using TLC. After completion the reaction, the solvent removed in vacuo, the residue co-evaporated twice with dichloromethane and the products obtained were crystallized from ethanol (20 mL) (Scheme 1).

(1, 3-Dioxoisoindolin-2-yl)methyl methylcarbamodithioate (**8a**): Color: White crystals. Yield: 72%. M.p.: 135-137 °C. FT-IR (KBr, ν, cm^{-1}): 3466 (NH broad), 3056 (Ar CH), 2997, 2930 (CH_2), 1772, 1715 (2 CO sharp), 1072 (CS sharp). ^{1}H NMR (400 MHz, DMSO-d_6, δ, ppm): 3.03 (d, 3H, *J* = 2.7 Hz, CH_3), 5.45 (s, 2H, NCH_2S), 7.86-7.93 (m, 4H, H_{arom}), 10.03 (s, 1H, NH). ^{13}C NMR (100 MHz, DMSO-d_6, δ, ppm): 30.71 (CH_3), 42.20 (NCH_2S), 123.44, 131.00, 134.87 (Aryl), 167.00 (2 × C=O), 193.00 (C=S). HRMS (ESI, *m/z*) calcd. for $C_{11}H_{10}N_2O_2S_2Na^+$ [M+Na]$^+$: 289.0080, Found: 289.0076.

(1, 3-Dioxoisoindolin-2-yl)methyl propylcarbamodithioate (**8b**): Color: Pale yellow crystals. Yield: 65%. M.p.: 144-146 °C. FT-IR (KBr, ν, cm^{-1}): 3293 (NH broad), 3062 (ArCH), 2961, 2918 (CH_2), 1762, 1710 (2 CO sharp), 1072 (CS sharp). ^{1}H NMR (400 MHz, DMSO-d_6, δ, ppm): 0.85-0.90 (t, 3H, CH_3), 1.52-1.63 (m, 2H, CH_3CH_2), 3.31-3.56 (m, 2H, $CH_3CH_2CH_2$), 5.45 (s, 2H, NCH_2S), 7.85-7.93 (m, 4H, H_{arom}), 10.04 (s, 1H, NH). ^{13}C NMR (100 MHz, $CDCl_3$, δ, ppm): 11.15 (CH_3), 20.98 (CH_3CH_2), 40.33 (NCH_2S), 48.86 ($CH_3CH_2CH_2$), 123.62, 131.16, 134.46

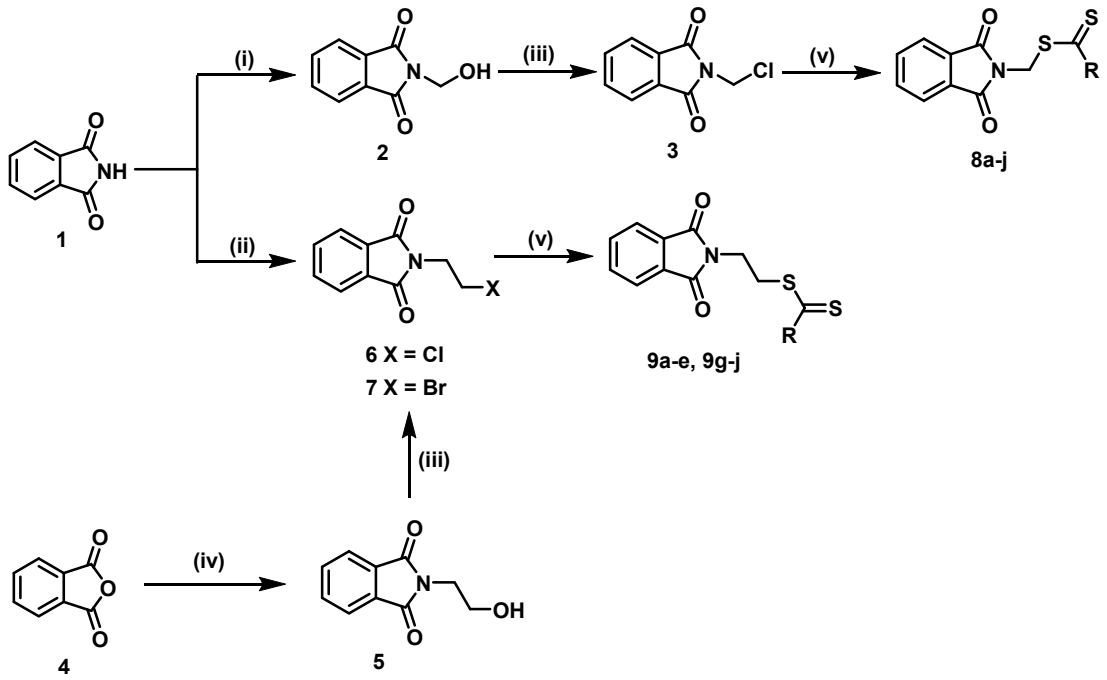

Reagents and conditions: (i) Formaldehyde (37% solution in water), reflux, 1 h; (ii) a) KOH, EtOH, b) $BrCH_2CH_2Br$; (iii) thionyl chloride, DMF, 0 °C, 1 h; (iv) Ethanolamine, EtOH, reflux; (v) RCS_2H, CH_3CN, room temperature, 48 h.

Scheme 1

(aryl), 167.16 (2 × C=O), 192.29 (C=S). HRMS (ESI, *m/z*) calcd. for $C_{13}H_{14}N_2O_2S_2Na^+$ [M+Na]$^+$: 317.0390, Found: 317.0389.

(1,3-Dioxoisoindolin-2-yl)methyl bis(2-hydroxyethyl)carbamodithioate (**8c**): Color: White crystals. Yield: 77%. M.p.: 100-102 °C. FT-IR (KBr, ν, cm^{-1}): 3374 (OH broad), 2932, 2879 (CH_2), 1773, 1718 (2 CO sharp), 1071 (CS sharp). ^{1}H NMR (400 MHz, DMSO-*d*$_6$, δ, ppm): 3.58-3.77 (m, 4H, CH_2NCH_2), 3.83-3.87 (m, 2H, CH_2OH), 4.07-4.11 (m, 2H, CH_2OH), 4.86-4.90 (m, 1H, OH), 4.96-5.02 (m, 1H, OH), 5.42 (s, 2H, NCH_2S), 7.83-7.93 (m, 4H, H_{arom}). ^{13}C NMR (100 MHz, $CDCl_3$, δ, ppm): 44.09 (NCH_2S), 57.69, 58.87 (2 × CH_2N), 60.53 (CH_2OH), 123.63, 131.82, 134.30 (aryl), 166.92 (2 × C=O), 195.60 (C=S). HRMS (MALDI, *m/z*) calcd. for $C_{14}H_{17}N_2O_4S_2^+$ [M+H]$^+$: 341.0630, Found: 341.0624.

(1, 3-Dioxoisoindolin-2-yl)methyl diethylcarbamodithioate (**8d**): Color: Colorless crystals. Yield: 65%. M.p.: 128-130 °C. FT-IR (KBr, ν, cm^{-1}): 2971, 2932 (CH_2), 1773, 1718 (2 CO sharp), 1064 (CS sharp). ^{1}H NMR (400 MHz, $CDCl_3$, δ, ppm): 1.23-1.28 (m, 6H, 2 × CH_3), 3.65 (q, 2H, *J* = 12 Hz, CH_2NCH_2), 4.01 (q, 2H, *J* = 12 Hz, CH_2NCH_2), 5.63 (s, 2H, NCH_2S), 7.72-7.75 (m, 2H, H_{arom}), 7.85-7.88 (m, 2H, H_{arom}). ^{13}C NMR (100 MHz, $CDCl_3$, δ, ppm): 11.50 (CH_3), 12.57 (CH_3), 43.83 (NCH_2S), 46.87, 49.34 (2 × CH_2NCH_2), 123.60, 131.93, 134.25 (aryl), 166.88 (2 ×C=O), 192.27 (C=S). HRMS (ESI, *m/z*) calcd. for $C_{14}H_{16}N_2O_2S_2Na^+$ [M+Na]$^+$: 331.0551, Found: 331.0545.

(1, 3-Dioxoisoindolin-2-yl)methyl cyclohexylcarbamodithioate (**8e**): Color: White crystals. Yield: 60%. M.p.: 185-187 °C. FT-IR (KBr, ν, cm^{-1}): 3283 (NH broad), 2934, 2853 (CH_2), 1767, 1712 (2 CO sharp), 1075 (CS sharp). ^{1}H NMR (400 MHz, $CDCl_3$, δ, ppm): 1.19-1.84 (m, 10H, cyclohex. $C_{2,3,4,5,6}$-H), 2.11-2.20 (m, 1H, cyclohex. C_1-H), 5.13 (s, 2H, NCH_2S), 7.75-7.80 (m, 2H, H_{arom}), 7.89-7.92 (m, 2H, H_{arom}), 8.30 (br s, 1H, NH). ^{13}C NMR (100 MHz, DMSO-*d*$_6$, δ, ppm): 23.75 (cyclohex. C_4), 24.61 (cyclohex. C_3), 25.04 (cyclohex. C_5), 30.31 (cyclohex. C_2), 30.88 (cyclohex. C_6), 41.08 (NCH_2S), 55.95 (cyclohex. C_1), 123.45, 131.39, 134.88 (aryl), 166.70 (2 × C=O), 191.26 (C=S). HRMS (MALDI, *m/z*) calcd. for $C_{16}H_{19}N_2O_2S_2^+$ [M+H]$^+$: 335.0888, Found: 335.0883.

(1, 3-Dioxoisoindolin-2-yl)methyl 2-(piperidin-1-yl)ethylcarbamodithioate (**8f**): Color: Yellow solid. Yield: 79%. M.p.: 143-146 °C. FT-IR (KBr, ν, cm^{-1}): 3438 (NH broad), 2929 (CH_2), 1772, 1718 (2 CO sharp), 1071 (CS sharp). ^{1}H NMR (400 MHz, DMSO-*d*$_6$, δ, ppm): 1.74-1.78 (m, 6H, pip. $C_{3,4,5}$-H), 2.48-2.49 (m, 4H, pip. $C_{2,6}$-H), 3.25-3.27 (m, 2H, CH_2N) 3.40-3.45 (m, 2H, $NHCH_2$), 5.47 (s, 2H, NCH_2S), 7.86-7.93 (m, 4H, H_{arom}), 10.51 (s, 1H, NH). ^{13}C NMR (100 MHz, DMSO-*d*$_6$, δ, ppm): 21.20 (pip. C_4), 22.36 (pip. C_3, C_5), 40.99 ($NHCH_2$), 41.36 (NCH_2S), 52.29 (CH_2N), 53.46 (pip. C_2, C_6), 123.59, 131.50, 135.05 (aryl), 166.83 (2 × C=O), 194.62 (C=S). HRMS (ESI, *m/z*) calcd. for $C_{17}H_{22}N_3O_2S_2^+$ [M+H]$^+$: 364.1153, Found: 364.1148.

(1, 3-Dioxoisoindolin-2-yl)methyl morpholinocarbamodithioate (**8g**): Color: White solid. Yield: 92%. M.p.: 198-200 °C. FT-IR (KBr, ν, cm^{-1}): 3435 (NH broad), 3098 (Ar CH), 2968, 2836 (CH_2), 1773, 1724 (2 CO sharp), 1039 (CS sharp). ^{1}H NMR (400 MHz, DMSO-*d*$_6$, δ, ppm): 2.79 (m, 4H, morph. $C_{3,5}$-H), 3.66 (m, 4H, morph. $C_{2,6}$-H), 5.27 (s, 2H, NCH_2S), 7.85-7.92 (m, 4H, H_{arom}), 9.67 (br s, 1H, NH). ^{13}C NMR (100 MHz, DMSO-*d*$_6$, δ, ppm): 40.08 (NCH_2S), 53.82 (morph. C_3, C_5), 65.64 (morph. C_2, C_6), 123.36, 131.45, 134.78 (aryl), 166.76 (2 × C=O), 196.33 (C=S). HRMS (ESI, *m/z*) calcd. for $C_{14}H_{16}N_3O_3S_2^+$ [M+H]$^+$: 338.0633, Found: 338.0628.

(1, 3-Dioxoisoindolin-2-yl)methyl 4-methylpiperazin-1-ylcarbamodithioate (**8h**): Color: White crystals. Yield: 72%. M.p.: 142-144 °C. FT-IR (KBr, ν, cm^{-1}): 3477 (NH broad), 3088 (Ar CH), 2925, 2888 (CH_2), 1773, 1721 (2 CO sharp), 1072 (CS sharp). ^{1}H NMR (400 MHz, DMSO-*d*$_6$, δ, ppm): 2.17 (s, 3H, CH_3), 2.19-2.24 (m, 4H, pip. $C_{3,5}$-H), 2.79 (brs, 4H, pip. $C_{2,6}$-H), 5.27 (s, 2H, NCH_2S), 7.84-7.92 (m, 4H, H_{arom}), 11.12 (s, 1H, NH). ^{13}C NMR (100 MHz, DMSO-*d*$_6$, δ, ppm): 40.06 (CH_3), 45.20 (NCH_2S), 53.07 (pip. C_3, C_5), 53.87 (pip. C_2, C_6), 123.34, 131.45, 134.75 (aryl), 166.76 (2 × C=O), 196.31 (C=S). HRMS (ESI, *m/z*) calcd. for $C_{15}H_{19}N_4O_2S_2^+$[M+H]$^+$: 351.0949, Found: 351.0942.

(1, 3-Dioxoisoindolin-2-yl)methyl piperidine-1-carbodithio ate (**8i**): Color: Colorless crystals. Yield: 63%. M.p.: 129-130 °C. FT-IR (KBr, ν, cm^{-1}): 2931, 2855 (CH_2), 1776, 1715 (2 CO sharp), 1071 (CS sharp). ^1H NMR (400 MHz, DMSO-d_6, δ, ppm): 1.57-1.64 (m, 6H, pip. $C_{3,4,5}$-H), 3.82 (br s, 2H, pip. C_2-H), 4.19 (br s, 2H, pip. C_6-H), 5.43 (s, 2H, NCH_2S), 7.84-7.93 (m, 4H, H_{arom}). ^{13}C NMR (100 MHz, $CDCl_3$, δ, ppm): 24.17 (pip. C_4), 25.99 (pip. C_3), 26.10 (pip. C_5), 43.85 (NCH_2S), 52.62 (pip. C_2), 52.90 (pip. C_6), 123.58, 131.92, 134.24 (aryl), 166.86 (2×C=O), 192.16 (C=S). HRMS (MALDI, *m/z*) calcd. for $C_{15}H_{17}N_2O_2S_2^+$ $[M+H]^+$: 321.0731, Found: 321.0722.

(1, 3-Dioxoisoindolin-2-yl)methyl morpholine-4-carbodithio ate (**8j**): Color: White solid. Yield: 88%. M.p.: 179-181 °C. FT-IR (KBr, ν, cm^{-1}): 2905, 2855 (CH_2), 1771, 1720 (2 CO), 1105 (CS sharp). ^1H NMR (400 MHz, DMSO-d_6, δ, ppm): 3.10-3.13 (m, 2H, morph. C_3-H), 3.65 (m, 2H, morph. C_5-H), 3.75-3.78 (m, 2H, morph. C_2-H), 4.27-4.30 (m, 2H, morph. C_6-H), 5.46 (s, 2H, NCH_2S), 7.87-7.93 (m, 4H, H_{arom}). ^{13}C NMR (100 MHz, DMSO-d_6, δ, ppm): 43.22 (NCH_2S), 63.52 (morph. C_3, C_5), 66.10 (morph. C_2, C_6), 123.47, 131.39, 134.91 (aryl), 166.60 (2 × C=O), 192.54 (C=S). HRMS (ESI, *m/z*) calcd. for $C_{14}H_{14}N_2O_3S_2Na^+$ $[M+Na]^+$: 345.0344, Found: 345.0338.

2-(1,3 -Dioxoisoindolin-2-yl)ethyl methylcarbamodithioate (**9a**): Color: White crystals. Yield: 75%. M.p.: 106-108 °C. FT-IR (KBr, ν, cm^{-1}): 3319 (NH broad), 3019 (Ar CH), 2930 (CH_2), 1766, 1705 (2 CO sharp), 1080 (CS sharp). ^1H NMR (400 MHz, DMSO-d_6, δ, ppm): 2.98-2.99 (m, 3H, CH_3), 3.49-3.52 (m, 2H, CH_2S), 3.84-3.88 (m, 2H, NCH_2), 7.82-7.88 (m, 4H, H_{arom}), 9.93 (s, 1H, NH). ^{13}C NMR (100 MHz, DMSO-d_6, δ, ppm): 32.44 (CH_3), 33.76 (NCH_2), 36.86 (CH_2S), 123.26, 131.52, 134.67 (aryl), 167.66 (2 × C=O), 195.33 ppm (C=S). HRMS (ESI, *m/z*) calcd. for $C_{12}H_{12}N_2O_2S_2Na^+$ $[M+Na]^+$: 303.0238, Found: 303.0232.

2-(1, 3-Dioxoisoindolin-2-yl)ethyl propylcarbamodithioate (**9b**): Color: White crystals. Yield: 61%. M.p.: 120-122 °C. FT-IR (KBr, ν, cm^{-1}): 3311 (NH broad), 2965, 2933, 2871 (CH_2), 1769, 1706 (2 CO sharp), 1072 (CS sharp). ^1H NMR (400 MHz, DMSO-d_6, δ, ppm): 0.80-0.85 (m, 3H, CH_3), 1.45-1.57 (m, 2H, CH_2), 3.44-3.60 (m, 4H, NHC*H*$_2$, CH_2S), 3.84-3.94 (m, 2H, NCH_2), 7.81-7.87 (m, 4H, H_{arom}), 9.96 (s, 1H, NH). ^{13}C NMR (100 MHz, DMSO-d_6, δ, ppm): 11.34 (CH_3), 20.82 (CH_3CH_2), 32.27 (NCH_2), 36.93 (CH_2S), 48.51($NHCH_2$), 123.07, 131.55, 134.44 (aryl), 167.65 (2 × C=O), 194.70 (C=S). HRMS (ESI, *m/z*) calcd. for $C_{14}H_{16}N_2O_2S_2Na^+$ $[M+Na]^+$: 331.0551, Found: 331.0545.

2-(1, 3-Dioxoisoindolin-2-yl)ethyl bis(2-hydroxyethyl)carba modithioate (**9c**): Color: White solid. Yield: 82%. M.p.: 93-95 °C. FT-IR (KBr, ν, cm^{-1}): 3371 (OH broad), 2955, 2857 (CH_2), 1768, 1704 (2 CO sharp), 1073 (CS sharp). ^1H NMR (400 MHz, DMSO-d_6, δ, ppm): 3.55-3.64 (m, 6H, CH_2NCH_2, CH_2S), 3.83-3.91 (m, 4H, 2 × C*H*$_2$OH), 4.06 (t, 2H, *J* = 6 Hz, NCH_2), 4.81 (t, 1H, *J* = 6 Hz, OH), 4.96 (t, 1H, *J* = 6 Hz, OH), 7.81-7.85 (m, 4H, H_{arom}). ^{13}C NMR (100 MHz, $CDCl_3$, δ, ppm): 34.99 (NCH_2), 36.39 (CH_2S), 57.79 (CH_2NCH_2), 59.19 (CH_2NCH_2), 60.01 (CH_2OH), 60.33 (CH_2OH), 123.34, 131.86, 134.18 (aryl), 168.45 (2× C=O), 196.63 (C=S). HRMS (ESI, *m/z*) calcd. for $C_{15}H_{18}N_2O_4S_2Na^+$ $[M+Na]^+$: 377.0606, Found: 377.0600.

2-(1, 3-Dioxoisoindolin-2-yl)ethyl diethylcarbamodithioate (**9d**): Color: Colorless crystals. Yield: 83%. M.p.: 115-117 °C. FT-IR (KBr, ν, cm^{-1}): 2968, 2936 (CH_2), 1769, 1707 (2 CO sharp), 1082 (CS sharp). ^1H NMR (400 MHz, $CDCl_3$, δ, ppm): 1.21-1.26 (m, 6H, 2 × CH_3), 3.66-3.69 (m, 4H, 2 × CH_2), 3.99-4.06 (m, 4H, CH_2S, NCH_2), 7.70-7.73 (m, 2H, H_{arom}), 7.81-7.86 (m, 2H, H_{arom}). ^{13}C NMR (100 MHz, $CDCl_3$, δ, ppm): 11.47 (CH_3), 12.44 (CH_3), 34.81 (NCH_2), 37.00 (CH_2S), 46.79 (CH_2NCH_2), 49.65 (CH_2NCH_2), 123.23, 132.06, 133.90 (aryl), 168.04 (2× C=O), 193.92 (C=S). HRMS (MALDI, *m/z*) calcd. for $C_{15}H_{19}N_2O_2S_2^+$ $[M+H]^+$: 323.0888, Found: 323.0880.

2-(1, 3-Dioxoisoindolin-2-yl)ethyl cyclohexylcarbamodithio ate (**9e**): Color: White solid. Yield: 61%. M.p.: 114-115 °C. FT-IR (KBr, ν, cm^{-1}): 3317 (NH broad), 2937, 2852 (CH_2), 1760, 1717 (2 CO sharp), 1088 (CS sharp). ^1H NMR (400 MHz, DMSO-d_6, δ, ppm): 1.09-1.27 (m, 6H, cyclohex. $C_{3,4,5}$-H), 1.55-1.83 (m, 5H, cyclohex. $C_{1,2,6}$-H), 3.52 (t, 2H, *J* = 8 Hz, CH_2S), 3.87 (t, 2H, *J* = 8 Hz, NCH_2), 7.82-7.88 (m, 4H, H_{arom}), 9.86 (d, 1H, *J* = 8 Hz, NH). ^{13}C NMR (100 MHz, DMSO-d_6, δ, ppm): 24.56 (cyclohex. C_3, C_5), 25.01 (cyclohex. C_4), 30.84 (cyclohex. C_2, C_6), 32.14 (NCH_2), 36.90 (CH_2S), 55.84 (cyclohex. C_1), 123.03, 131.53, 134.39 (aryl), 167.59 (2 × C=O), 193.21 (C=S). HRMS (ESI, *m/z*) calcd. for $C_{17}H_{21}N_2O_2S_2^+$ $[M+H]^+$: 349.1044, Found: 349.1046.

2-(1, 3-Dioxoisoindolin-2-yl)ethyl morpholinocarbamodithio ate (**9g**): Color: White solid. Yield: 78%. M.p.: 208-210 °C. FT-IR (KBr, ν, cm^{-1}): 3208 (NH broad), 2961, 2917 (CH_2), 1765, 1704 (2 CO sharp), 1035 (CS sharp). ^1H NMR (400 MHz, DMSO-d_6, δ, ppm): 2.75 (m, 4H, morph. $C_{3,5}$-H), 3.09-3.11 (m, 2H, morph. C_2-H), 3.39-3.43 (m, 2H, CH_2S), 3.64-3.76 (m, 2H, morph. C_6-H), 3.85-3.89 (m, 2H, NCH_2), 7.81-7.88 (m, 4H, H_{arom}), 10.99 (s, 1H, NH). ^{13}C NMR (100 MHz, DMSO-d_6, δ, ppm): 30.61 (NCH_2), 36.85 (CH_2S), 42.86 (morph. C_3), 53.69 (morph. C_5), 63.26 (morph. C_2), 65.66 (morph. C_6), 123.00, 131.58, 134.40 (aryl), 167.69 (2 × C=O), 198.21 (C=S). HRMS (ESI, *m/z*) calcd. for $C_{15}H_{18}N_3O_3S_2^+$ $[M+H]^+$: 352.0790, Found: 352.0784.

2-(1, 3-Dioxoisoindolin-2-yl)ethyl 4-methylpiperazin-1-ylcar bamodithioate (**9h**): Color: White solid. Yield: 64%. M.p.: 119-121 °C. FT-IR (KBr, ν, cm^{-1}): 3462 (NH broad), 2941, 2811 (CH_2), 1775, 1724 (2 CO sharp), 1040 (CS sharp). ^1H NMR (400 MHz, DMSO-d_6, δ, ppm): 2.18 (s, 3H, CH_3), 2.33 (brs, 4H, pip. $C_{3,5}$-H), 3.59-3.63 (m, 2H, CH_2S), 3.86-3.91 (m, 4H, pip. C_2-H, NCH_2), 4.17 (brs, 2H, pip. C_6-H), 7.82-7.88 (m, 4H, H_{arom}), 10.85 (s, 1H, NH). ^{13}C NMR (100 MHz, DMSO-d_6, δ, ppm): 34.25 (NCH_2), 36.63 (CH_2S), 45.04 (NCH_3), 53.84 (pip. C_3, C_5, C_2, C_6), 123.07, 131.52, 134.44 (aryl), 167.62 (2 × C=O), 193.91 (C=S). HRMS (ESI, *m/z*) calcd. for $C_{16}H_{21}N_4O_2S_2^+$ $[M+H]^+$: 365.1106, Found: 365.1095.

2-(1, 3-Dioxoisoindolin-2-yl)ethyl piperidine-1-carbodithio ate (**9i**): Color: Colorless crystals. Yield: 85%. M.p.: 170-172 °C. FT-IR (KBr, ν, cm^{-1}): 2932, 2854 (CH_2), 1767, 1707 (2 CO sharp), 1082 (CS sharp). ^1H NMR (400 MHz, DMSO-d_6, δ, ppm): 1.51-1.65 (m, 6H, pip. $C_{3,4,5}$-H), 2.99-3.03 (m, 2H, pip. C_2-H), 3.58 (m, 2H, CH_2S), 3.84 (m, 3H, pip. C_6-H, NCH_2), 4.15 (brs, 1H, pip. C_6-H), 7.81-7.87 (m, 4H, H_{arom}). ^{13}C NMR (100 MHz, DMSO-d_6, δ, ppm): 21.61 (pip. C_4), 22.16 (pip. C_3), 23.54 (pip. C_5), 34.30 (NCH_2), 37.55 (CH_2S), 43.71 (pip. C_2, C_6), 123.06, 131.55, 134.46 (aryl), 167.69 (2 × C=O), 192.52 (C=S). HRMS (ESI, *m/z*) calcd. for $C_{16}H_{18}N_2O_2S_2Na^+$ $[M+Na]^+$: 357.0707, Found: 357.0700.

2-(1, 3-Dioxoisoindolin-2-yl)ethyl morpholine-4-carbodithio ate (**9j**) [23]: Color: White solid. Yield: 84%. M.p.: 176-178 °C. FT-IR (KBr, ν, cm^{-1}): 2849 (CH_2), 1714, 1417 (2 CO sharp), 1104 (CS sharp). ^1H NMR (400 MHz, $CDCl_3$, δ, ppm): 3.69-3.75 (m, 6H, morph. $C_{3,5}$-H, CH_2S), 3.90-4.08 (m, 6H, morph. $C_{2,6}$-H, NCH_2), 7.69-7.73 (m, 2H, H_{arom}), 7.83-7.87 (m, 2H, H_{arom}). ^{13}C NMR (100 MHz, $CDCl_3$, δ, ppm): 34.81 (NCH_2), 36.80 (CH_2S), 51.12 (morph. C_3, C_5), 66.19 (morph. C_2, C_6), 123.29, 132.00, 134.00 (aryl), 168.04 (2 × C=O), 195.86 (C=S). HRMS (MALDI, *m/z*) calcd. for $C_{15}H_{17}N_2O_3S_2^+$ $[M+H]^+$: 337.0681, Found: 337.0694.

2.3. Biological evaluation

2.3.1. Antiproliferation assay

Human breast adenocarcinoma MCF-7 cells, hepatocellular carcinoma HepG2 cells, colon carcinoma HCT-116 cells, cervical carcinoma HeLa cells and alveolar adenocarcinoma A549 cells were purchased from American Type Culture Collection (ATCC, Rockville, MD, USA). HepG2, MCF-7, A549 and HeLa cells were routinely cultured in Dulbecco's Modified Eagle's Medium (DMEM), while HCT-116 cells were cultured in McCoy's medium. Media were supplemented with 2 mM L-glutamine, 100 units/mL penicillin G sodium, 250 ng/mL

amphotericin B, 100 units/mL streptomycin sulphate, and 10% fetal bovine serum (FBS). Cells were maintained in 37 °C humidified air containing 5% CO_2 at sub-confluence. Cells were harvested when confluence had reached 75% using trypsin/EDTA. All cell culture materials were obtained from Gibco®/Invitro gen, USA. All chemicals were obtained from Sigma/Aldrich, USA, except the mentioned.

The antiproliferative activity of phthalimide derivatives against Hep-G2, MCF-7, HCT-116, A549, and HeLa cells was estimated by 3-(4,5-dimethylthiazol-2-yl)-2,5-diphenyl-tetra zolium bromide (MTT) assay [24]. Briefly, cells were seeded in 96-well plates at 5×10^4 cells/well in the corresponding media supplemented with culture materials mentioned above. After 24 h of culture, phthalimide derivatives were individually added in triplicate in a range of 12.5-1000 μM, and the cells were further cultured for 24 h. The cells were then exposed to MTT (5 mg/mL in PBS) at a final concentration of 1 mg/mL in culture for 4 h. Formazan crystals formed during the incubation period were dissolved overnight at 37 °C by adding 10% SDS containing 0.02 N HCl. The absorbance was then measured at 570 nm (FLUOstar OPTIMA; BMG Labtech GmbH, Offenburg, Germany). The half maximal growth inhibitory concentration (IC_{50} values) was calculated from the dose-dependent curve equation of each compound. The experiment was repeated three times. Thalidomide was used as drug of reference (**TH**).

2.3.2. Molecular docking study

Molecular modeling study was performed using Accelrys Discovery Studio 2.5 operating system (Accelrys Inc., San Diego, CA, USA), at Faculty of Pharmacy, Ain-Shams University, Cairo, Egypt. Molecules were built within Docking Study (DS) and conformational models for each compound were generated automatically. Docking study involved the following steps: The docking analysis was carried out on VEGFR enzyme. The 3D protein structure of VEGFR enzyme co-crystallized with lead compound (Code; 2OH4), was downloaded from the Protein Data Bank of the Research Collaboration for Structural Bioinformatics (RCSB) website www.rcsb.org. The binding pocket was prepared for docking by cleaning the protein, adding the missing hydrogen and side chains and energy minimization according to DS protocol. The binding pocket of the complexed lead compound with the connected amino acid residues was identified at sphere of radius = 12 Å and then was used in docking of test compounds using Genetic Optimization for Ligand Docking (GOLD) module. After that the GOLD score fitness of the best fitted conformation of the docked molecule were recorded.

2.3.3. Estimation of compound's binding affinity to VEGFR

The direct binding of pure compounds to VEGFR protein were tested in cell-free ELISA to discover the possible direct compound/receptor binding that may block the receptor. The assay was mainly examining the possible binding between each compound to the antigenic determinant sequence in the VEGFR protein that can prevent its further binding to VEGFR antibodies. In brief, each pure compound (10 mg/mL) was incubated with a fixed concentration of recombinant human VEGFR (0.5 ng/mL, Abcam, USA) at 37 °C for 1h under orbital shaking in non-coated microplates. After incubation, the compound/receptor mixture was transferred to ELISA-microplates that were previously coated with VEGFR monoclonal antibodies and the level of free VEGFR protein was quantified by sandwich ELISA as previously mentioned [25].

2.3.4. Statistical analysis

Statistical analyses of data were performed using the Statistical Package for the Social Sciences (SPSS) program Version 11 and one way ANOVA test followed by Tuckey's Post Hoc test. Data were expressed as mean±standard division (SD). The results were considered to be significant when p value is less than 0.05.

3. Results and discussion

3.1. Chemistry

Merging the bridgeheads of different dithiocarbamate and dithioate moieties to phthalimide is the core of our rational design of a series of novel dithiocarbamate phthalimide hybrids (**8a-j**, **9a-e**, **9g-j**). The novel phthalimide derivatives were synthesized according to the procedures depicted in Scheme 1. Phthalimide (**1**) with its (NH) acidic hydrogen underwent reaction with formaldehyde affording the intermediate hydroxymethyl derivative **2** that was subjected to chlorination using thionyl chloride to furnish the chloromethylene derivative **3** with perfect yields according to the reported procedure [26]. Similarly, *N*-chloroethylene phthalimide derivative could be prepared by condensation of phthalic anhydride (**4**) with ethanolamine to construct the hydroxyethyl derivative **5** that is to be subsequently halogenated to afford chloroethyl derivative **6** [27-29]. Alternatively, *N*-bromoethylene phthalimide derivative could be prepared by the reaction of phthalimide **1** with potassium hydroxide to afford potassium phthalimide which reacted with ethylene dibromide to give bromoethyl derivative **7** [30]. In the current study, the commercially available bromoethylene counterpart **7** has been utilized for the synthesis of the ethylene bridged analogs. *N*-Chloromethylphthalimide (**3**) and *N*-bromoethyl-phthalimide (**7**) were allowed to react with CS_2 and different amines under stirring for 48 h at room temperature in CH_3CN to afford novel phthalimide dithiocarbamate and dithioate derivatives (**8a-j**, **9a-e**, **9g-j**). Phthalimide derivative **9f** failed to proceed properly and no indication for its formation was achieved. The structures of amines applied in this reaction protocol are given in Table 1. The chemical structures of the synthesized compounds were confirmed by IR, ^{1}H NMR, ^{13}C NMR, and Electrospray ionization high resolution mass spectra (ESI-HRMS). The IR spectra of phthalimide dithiocarbamate derivatives **8a-j**, **9a-e** and **9g-j** supported the expected structures and showed absorption bands in the region 1704-1776 cm^{-1} as two peaks owing to asymmetric and symmetric stretching vibrations of the two carbonyls of phthalimide. The IR spectra of phthalimide dithiocarbamate and dithioate derivatives **8a-j**, **9a-e** and **9g-j** showed absorption bands in the 1035-1088 cm^{-1} region resulting from C=S function. ^{1}H NMR spectra of phthalimide dithiocarbamate and dithioate derivatives **8a-j** showed singlets at δ 5.13-5.63 ppm corresponding to the methylene protons (N-CH_2-S). ^{13}C NMR spectra of phthalimide dithiocarbamate and dithioate derivatives **8a-j** showed signals at δ 40.08-45.20 ppm corresponding to the methylene carbon (N-CH_2-S). On the other hand, ^{1}H NMR spectra of phthalimide dithiocarbamate and dithioate derivatives **9a-e** and **9g-j** showed triplet at δ 3.44-3.75 ppm corresponding to the methylene proton (CH_2S), triplet at δ 3.84-4.08 ppm corresponding to (N-CH_2). These two triplets in some of synthesized compounds appeared as multiplet due to the overlap with protons for the derivatized amine side chain. Similarly, ^{13}C NMR spectra of phthalimide dithiocarbamate and dithioate derivatives **9a-e** and **9g-j** showed signals at δ 30.61-34.99 ppm corresponding to (N-CH_2), signals at 36.39-37.35 ppm corresponding to (CH_2S). In addition, ^{13}C NMR spectra of all compounds showed signals at δ 191.26-198.21 ppm corresponding to (C=S). ESI-HR mass spectra of phthalimide dithiocarbamate and dithioate derivatives **8a-j**, **9a-e** and **9g-j**, respectively, displayed molecular ions (M^+), which confirmed their molecular weights. All the analytical data were in complete accordance with the proposed structures. Reagents and analytical data are presented in Experimental part.

Table 1. Appropriate amine and corresponding phthalimide dithiocarbamate and dithioate derivatives.

Amine	Product	Structure	Product	Structure
CH_3NH_2	8a	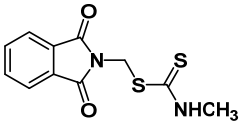	9a	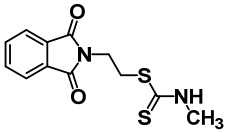
$CH_3CH_2CH_2NH_2$	8b	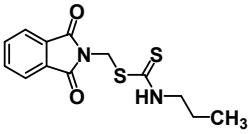	9b	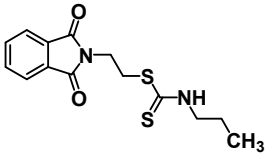
$HOCH_2CH_2NH_2$	8c	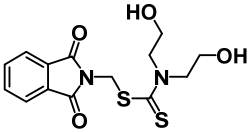	9c	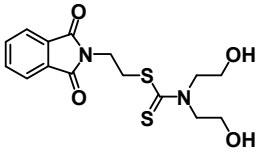
$(CH_3CH_2)_2NH$	8d	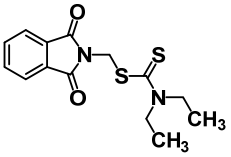	9d	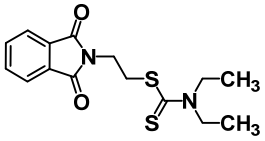
	8e	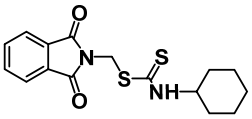	9e	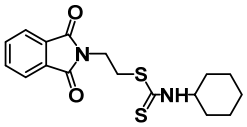
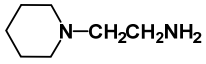	8f	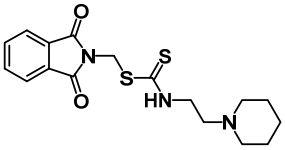	9f	Not proceed
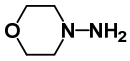	8g	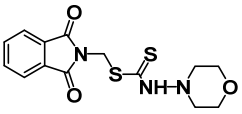	9g	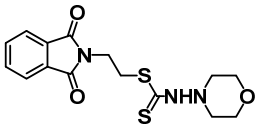
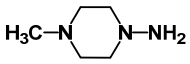	8h	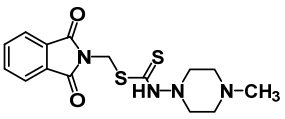	9 h	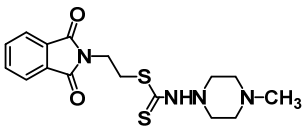
	8i	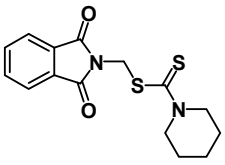	9i	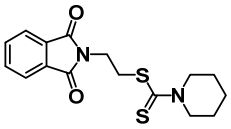
	8j	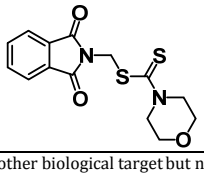	9j[a]	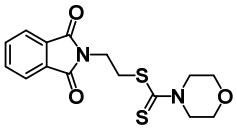

[a] Derivative **9j** was previously reported for another biological target but not characterized [23].

3.2. Biological evaluation

3.2.1. Effect of phthalimide derivatives on proliferation of human cancer cells

The antiproliferative effects of the newly synthesized phthalimide derivatives were tested against MCF-7, HepG2, HCT-116, cervical carcinoma HeLa, A549 cells by using MTT assay. Phthalimide derivatives were dissolved in dimethyl-sulphoxide (DMSO), and then diluted 1000 times for the assays. The solubility and absence of crystals as well as precipitation were analyzed under microscope after dilution of compounds/DMSO in their corresponding culture media.

Table 2. Antiproliferative activity of phthalimide derivatives on different human cancer cells *.

Compounds	MCF-7	HepG2	HCT-116	HeLa	A549
TH	131.9	207.3	361.8	227.3	144.1
8c	514.6	236.37	741.3	846.5	552.4
8e	534.4	412.5	486.1	555.1	362.2
8f	608.5	207.2	156.9	179.1	553.6
8g	424.4	342.5	273.6	312.4	223.8
8h	493.3	256.4	539.0	615.6	401.7
8i	482.8	411.6	373.3	426.4	278.2
9c	501.4	269.9	425.7	486.1	317.2
9e	66.9	87.1	742.9	348.4	116.9
9i	132.0	151.9	273.2	426.1	178.1
9j	603.2	299.3	616.8	704.4	459.6

* Proliferation assay was determined by MTT assay and obtained from at least three independent experiments. Cells were treated for 24 h with phthalimide derivatives in concentration range 12.5-1000 μM. Data are presented as IC_{50} (μM), which were calculated from the exponential equation of dose/viability %response. Thalidomide was used as drug of reference (**TH**).

Table 3. Docking score for each compound in the test set with active site of VEGFR.

Compounds	GOLD score (-kcal/mol)
TH	44.45
8c	50.80
8e	51.37
8f	49.87
8g	50.98
8h	50.44
8i	46.63
9c	49.15
9e	54.40
9i	51.70
9j	45.98

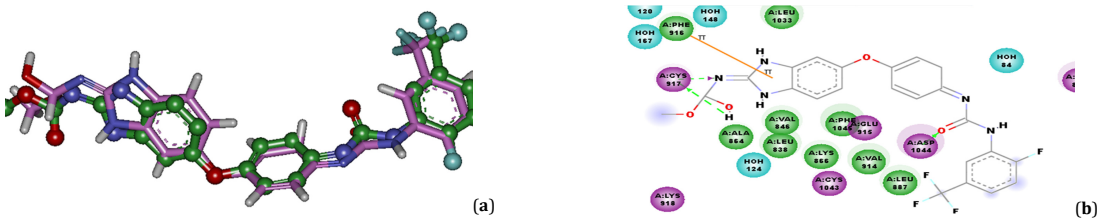

Figure 3. a) Alignment of bioactive conformer of lead from Pdb and docked conformer, b) 2D binding mode of lead compound.

Compounds **8a**, **8b**, **8d**, **8j**, **9a**, **9b**, **9d**, **9g** and **9h** that precipitated in cell culture media were omitted from biological evaluation experiments.

As shown in Table 2, our results indicated that in MCF-7 cells, compound **9e** possessed the highest antiproliferative activity (IC_{50} = 66.9 μM), whereas, derivative **9i** showed similar antiproliferative effect with **TH** (IC_{50} about 132 μM). In HepG2 cells, derivatives **9e** and **9i** exhibited the maximum antiproliferative effect with IC_{50} = 87.1 μM and 151.9 μM, respectively, compared to **TH** (IC_{50} = 207.3 μM). Moreover, in lung A549 cells, all of the tested derivatives showed non-antiproliferative activity with IC_{50} > 200 μM, except derivatives **9e** and **9i** which revealed antiproliferative activity (IC_{50} = 116.9 and 178.1 μM, respectively) compared to **TH** (IC_{50} = 144.1 μM). Furthermore, in both colon HCT-116 and cervical HeLa, only derivative **8f** showed antiproliferative effect with IC_{50} = 156.9 and 179.1 μM, respectively than **TH** (IC_{50} = 361.8 and 227.3 μM, respectively).

3.2.2. Molecular docking study

It was reported that **TH** and its analogs have VEGFR inhibitory activities [31-33]. Molecular docking investigated the affinity of the designed compounds into the active site of VEGFR enzyme (PDP: 2OH4) [34]. Both the binding modes and the docking scores of the designed target compounds compared to the lead compound were evaluated. The selection of pdb 2OH4 was based on similarity in structure between the designed compounds and the selected lead which proposed to have the same pharmacophoric features (Figure 3).

Interactive docking using GOLD protocol was carried out for all the conformers of each compound of the test set (**8c**, **8e**, **8f**, **8g**, **8h**, **8i**, **9c**, **9e**, **9i**, **9**j and **TH**) to the selected active site after energy minimization. The small RMSD values proved the validity of the used docking processes [35]. Each docked compound was assigned a score according to its binding mode onto the binding site [36] that predicted binding energies and the corresponding experimental values as outlined in Table 3.

The lead binding mode involved shows that NH attached to benzimidazole nucleus forms H-bond with the Cys917 in the hinge region. On the other hand, the benzimidazole nucleus forms hydrophobic interaction with Phe916 in the hinge region. Furthermore, the extended chains are solvated and occupied in the hydrophobic pocket [37,38]. Also, the binding mode of ATP was matched with the reported results [39]. All interaction behaviors, as obtained from the docking studies, were found to be in accordance with the reported binding mode of the VEGFR active site [37,38]. The active compounds elicited the same conformation of the lead compound with bioisosteric replacement of benzimidazole nucleus by isoindole nucleus and hence acquired the same binding mode of the lead. Derivatives **9e** and **9i**, which showed similar binding mode to the lead compound with high docking score values (-54.4 and -51.7 kcal/mol), revealed the highest inhibitory activity of 64.8 and 60.5%, respectively (Figures 4 and 5). The carbonyl group in the active hits (**9e** and **9i**) conserved the H-bond interaction with CYS917 in the hinge region and the extended chain occupied the hydrophobic pocket and solvated to form extra hydrogen bonding (Figures 4 and 5).

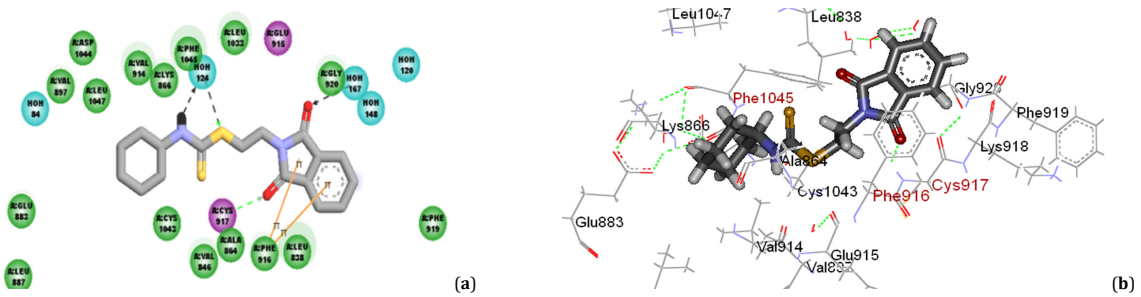

Figure 4. a) 2D and b) 3D interaction diagram of compound **9e** in the active site of VEGFR.

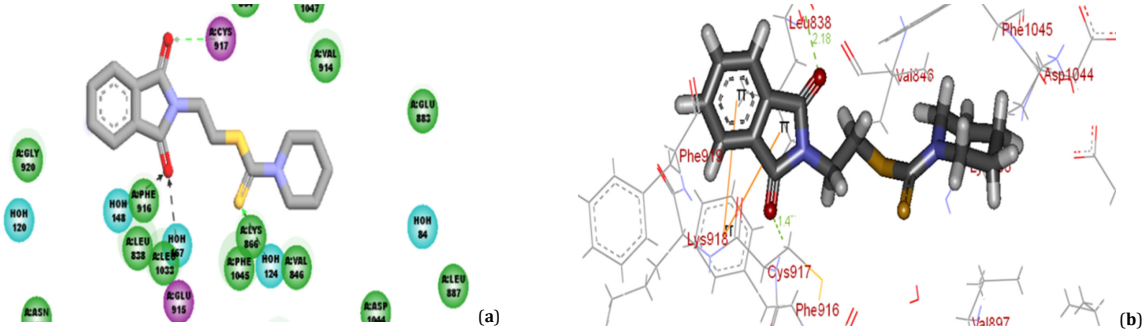

Figure 5. a) 2D and b) 3D alignment of compound **9i** having fitting score = -51.7 Kcal/mol and biological activity = 60.5%.

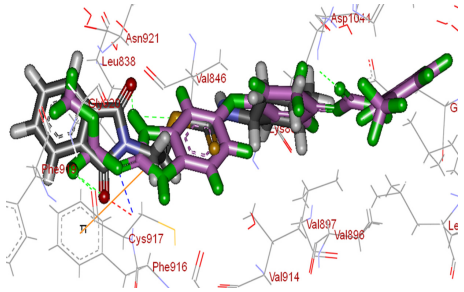

Figure 6. Alignment of compound **9e** (with grey color) and the lead compound (with purple color) in the active site of VEGFR.

Compared to lead compound (potent and selective VEGFR inhibitor), docking behavior with derivative **9e** exhibited that our constructed analog was perfectly aligned with the lead compound taking the same orientation of the features inside the active site (Figure 6). These observations support the attained structure activity relationship (SAR) assumptions due to enzymatic inhibitory activity data.

3.2.3. Assessment of phthalimide derivatives on VEGFR concentration

The present study explored the affinity of the prepared derivatives to directly bind the VEGFR protein molecule in the antigenic sequence that may lead to a change in its ability to bind VEGF. As shown in Figure 7, the results demonstrated that the incubation of recombinant human VEGFR with the tested derivatives resulted in a variable range of inhibition in the VEGFR detection by its corresponding antibodies. In descending order, derivatives **9e** > **9i** > **TH** were the most potent inhibitors of VEGFR detection, among all of the tested derivatives, at percentage of inhibition > 50%.

Finally, preliminary biological screening indicated that the nature of dithiocarbamate and dithioate moieties introduced at the phthalimide nitrogen atom play an important role in the potency of phthalimide derivatives **9e** and **9i** toward different biological targets. The outcome results of phthalimide derivatives **8f**, **9e** and **9i** revealed the superior relative activity of cyclohexylamine and piperidine side chains which supports our previously reported data using the same dithiocarbamate and dithioate moieties with thalidomide [8,11]. Moreover, the introduction of alkyl linker in between phthalimide and dithiocarbamate moieties in derivatives **9e** and **9i** added a value in improving their biological activities. These findings are in agreement with the previously reported investigations which stated that alkyl linkers could modulate the physicochemical properties and thus improve the biological potency [40-42].

4. Conclusion

Herein; we report the synthesis and biological evaluation of phthalimide moiety with different dithiocarbamate and dithioate side chains. The improvement of biological activities compared to thalidomide depends on the nature of dithiocarbamate and dithioate groups attached to phthalimide core and the presence of alkyl linker in between. Phthalimide derivatives **9e** and **9i** showed remarkable antitumor activities.

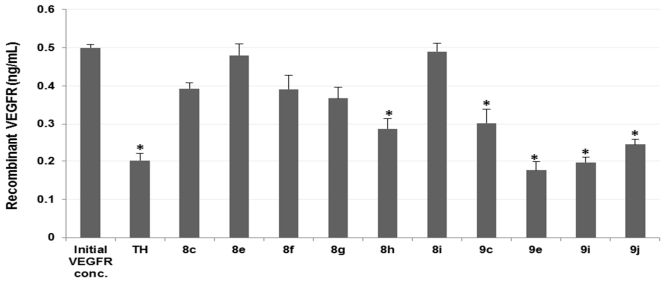

Figure 7. Effect of phthalimide derivatives on VEGFR concentration. The concentration of VEGFR was measured after the incubation of each tested phthalimide derivative (10 μg/mL) with a fixed concentration of the standard recombinant human VEGFR (0.5 ng/mL) using ELISA

The active hits exhibited the highest inhibitory activity on VEGFR enzyme which was consistent with biological findings and consequently lead to inhibition of tumor growth. These results suggest that piperidine and cyclohexylamine derivatives have potential promising activities. Future directions may include insertion of some other linkers of different lengths and functionalities in between phthalimide and dithiocarbamate moieties for further improvement the activity.

Acknowledgement

This research was supported by Science and Technology Development Fund (STDF) through Project No. 3627. The corresponding author and all the co-authors appreciate the Egyptian fund for supporting this research. We appreciate our thank to Prof. Erik Pedersen from department of Physics, Chemistry and Pharmacy, Nucleic Acid Center, University of Southern Denmark, Odense, Denmark for the scientific supporting this research.

References

[1]. Eger, K.; Jalalian, B.; Verspohl, E. J.; Lupke, N. P. *Arzneim Forsch* **1990**, *40*, 1073-1075.
[2]. Folkman, J. *Ann. Int. Med.* **1975**, *82*, 96-100.
[3]. Bartlett, J. B.; Dredge, K.; Dalgleish, A. G. *Nat. Rev. Cancer* **2004**, *4*, 314-322.
[4]. Juliussin, G.; Celsing, F.; Tursson, I.; Lenhoff, S.; Adriansson, M.; Malm, C. *Br. J. Haematol.* ***2000***, *109*, 89-96.
[5]. Hashimoto, Y. *Arch. Pharm.* **2008**, *341*, 536-547.
[6]. Chan, S. H.; Lam, K. H.; Chui, C. H.; Gambari, R.; Yuen, M. C.; Wong, R. S.; Cheng, G. Y.; Lau, F. Y.; Au, Y. K.; Cheng, C. H.; Lai, P. B.; Kan, C. W.; Lung-Kok, S. H.; Tang, J. C.; Chan, A. S. *Eur. J. Med. Chem.* **2009**, *44*, 2736-2740.
[7]. Sondhi, S. M.; Rani, R.; Roy, P.; Agrawal, S. K.; Saxena, A. K. *Bioorg. Med. Chem. Lett.* **2009**, *19*, 1534-1538.
[8]. Zahran, M. A.; Salem, T . A.; Samaka, R. M.; Agwa, H. S.; Awad, A. R. *Bioorg. Med. Chem.* **2008**, *16*, 9708-9718.
[9]. Guirgis, A. A.; Zahran, M. A.; Mohamed, A. S.; Talaat, R. M.; Abdou, B. Y.; Agwa, H. S. *Int. Immunopharmacol.* **2010**, *10*, 806-811.
[10]. Talaat, R.; El-Sayed, W.; Agwa, H.; Gamal-Eldeen, A. M.; Moawia, S.; Zahran, M. *Biomed. Aging. Pathol.* **2014**, *4*, 179-189.
[11]. Zahran, M.; Gamal-Eldeen, A. M.; El-Hussieny, E. A.; Agwa, H. *J. Genet. Eng. Biotech.* **2014**, *12*, 65-70.
[12]. El-Aarag, B. Y. A.; Kasai, T.; Zahran, M. A. -H.; Zakhary, N. I.; Shigehiro, T.; Sekhar, S. C.; Agwa, H. S.; Mizutani, A.; Murakami, H.; Kakuta, H.; Seno, M. *Int. Immunopharmacol.* **2014**, *21*, 283-292.
[13]. Talaat, R.; El-Sayed, W.; Agwa, H.; Gamal-Eldeen, A. M.; Moawia, S.; Zahran, M. *Chem. Biol. Interact.* **2015**, *238*, 74-81.
[14]. El-Aarag, B.; Kasai, T.; Masuda, J.; Agwa, H.; Zahran, M.; Seno, M. *Biomed. Pharmacother.* **2017**, *85*, 549-555.
[15]. Ronconi, L.; Marzano, C.; Zanello, P.; Corsini, M.; Miolo, G.; Macca, C.; Trevisan, A.; Fregona, D. *J. Med. Chem.* **2006**, *49*, 1648-1657.
[16]. Ozkirimli, S.; Apak, T. I.; Kiraz, M.; Yegenoglu, Y. *Arch. Pharm. Res.* **2005**, *28*, 1213-1218.
[17]. Huang, W.; Ding, Y.; Miao, Y.; Liu, M. Z.; Yang, G. F. *Eur. J. Med. Chem.* **2009**, *44*, 3687-3696.
[18]. Cao, S. L.; Feng, Y. P.; Jiang, Y. Y.; Liu, S. Y.; Ding, G. Y.; Li, R. T. *Bioorg. Med. Chem. Lett.* **2005**, *15*, 1915-1917.
[19]. Zahra, M.; Osman, A.; Agwa, H.; Nair, N.; Sanchez, A.; Hurley, L.; Farag, D.; Kasai, T.; Seno, M.; Zahran, M. *Med. Chem.* **2016**, *6(12),* 694-703.
[20]. Zahran, M.; Abdin, Y.; Salama, H. *Arkivoc* **2008**, *11*, 256-265.
[21]. Zahran, M.; Salama, H. F.; Abdin, Y. G.; Gamal-Eldeen, A. M. *J. Chem. Sci.* **2010**, *122*, 587-595.
[22]. Zahran, M. A.; Abdin, Y. G.; Osman, A. M.; Gamal-Eldeen, A. M.; Talaat, R. M.; Pedersen, E. B. *Arch. Pharm. Chem.* **2014**, *347*, 1-8.
[23]. Shaohua, G.; Wenkang, H.; Jian, Z.; Yonghua, W. *Bioorg. Med. Chem. Lett.* **2015**, *25*, 3464-3467.
[24]. Hansen, M. B.; Nielsen, S. E.; Berg, K. *J. Immunol. Methods* **1989**, *119*, 203-210.
[25]. Talaat, R. M. *Viral Immunol.* **2010**, *23*, 151-157.
[26]. Cho, S. D.; Hwang, J.; Kim, H. K.; Yim, H. S.; Kim, J. J.; Lee, S. G.; Yoon, Y. J. *J. Heterocycl. Chem.* **2007**, *44*, 951-960.
[27]. Fhid, O.; Doma, A. M.; Zeglam, T. H.; Baki, J.; Zitouni, M.; Sdera, W. *Der Pharma Chem.* **2015**, *7(11)*, 240-242.
[28]. Hess, S.; Akermann, M. A.; Wnendt, S.; Zwingenberger, K.; Eger, K. *Bioorg. Med. Chem.* **2001**, *9*, 1279-1291.
[29]. Norman, M. H.; Minick, D. J.; Rigdon, G. C. *J. Med. Chem.* **1996**, *39*, 149-157.
[30]. Salzberg, P. L.; Supniewski, J. V. *Org. Synth.* **1927**, *7*, 8-8.
[31]. Yabu, T.; Tomimoto, H.; Taguchi, Y.; Yamaoka, S.; Igarashi, Y.; Okazaki, T. *Blood* **2005**, *106 (1),* 125-134.
[32]. Rafiee, P.; Stein, D. J.; Nelson, V. M.; Otterson, M. F.; Shaker, R.; Binion, D. G. *Am. J. Physiol. Gastrointest. Liver Physiol.* **2010**, *298*, 167-176.
[33]. Prager, G. W.; Poettler, M.; Unseld, M.; Zielinski, C. C. *Transl. Lung Cancer Res.* **2012**, *1*, 14-25.
[34]. Hasegawa, M.; Nishigaki, N.; Washio, Y.; Kano, K.; Harris, P. A.; Sato, H.; Mori, I.; West, R. I.; Shibahara, M.; Toyoda, H.; Wang, L.; Nolte, R. T.; Veal, J. M.; Cheung, M. *J. Med. Chem.* **2007**, *50*, 4453-4470.
[35]. Elgazwy, A. S.; Ismail, N. S.; Elzahabi, H. S. *Bioorg. Med. Chem.* **2010**, *18*, 7639-7650.
[36]. Alley, M. C.; Scudiero, D. A.; Monks, A.; Hursey, M. L.; Czerwinski, M. J.; Fine, D. L.; Abbott, B. J.; Mayo, J. G.; Shoemaker, R. H.; Boyd, M. R. *Cancer Res.* **1988**, *48*, 589-601.
[37]. Kar, R. K.; Suryadevara, P.; Sahoo, B. R.; Sahoo, G. C.; Dikhit, M. R.; Das, P. *SAR QSAR Environ Res.* **2013**, *24*, 215-234.
[38]. Sharad, V.; Amit, S.; Abha, M. *J. Appl. Pharma. Sci.* **2012**, *2*, 41-46.
[39]. Paul, M. K.; Mukhopadhyay, A. K. *Int. J. Med. Sci.* **2004**, *1*, 101-115.
[40]. Krier, M.; Araujo-Junior, J. X.; Schmitt, M.; Duranton, J.; Justiano-Basaran, H.; Lugnier, C.; Bourguignon, J. J.; Rognan, D. *J. Med. Chem.* **2005**, *48*, 3816-3822.
[41]. Kamal, A.; Ramu, R.; Tekumalla, V.; Khanna, G. B.; Barkume, M. S.; Juvekar, A. S.; Zingde, S. M. *Bioorg. Med. Chem.* **2008**, *16*, 7218-7224.
[42]. Wang, X. L.; Wan, K.; Zhou, C. H. *Eur. J. Med. Chem.* **2010**, *45*, 4631-4639.